

TECHNICAL B-H SATURATION MAGNETIZATION CURVE MODELS FOR SPICE, FEM AND MoM SIMULATIONS

Submitted: 2nd February 2016; accepted 29th February 2016

Roman Szewczyk

DOI: 10.14313/JAMRIS_2-2016/10

Abstract:

Recent development of SPICE, FEM and MoM software often requires the fast and reliable description of BH saturation magnetization curve. In spite of the fact that physical models of BH saturation curve are very sophisticated, for technical purposes, such curve may be modelled by simplified equations.

Paper presents the quantitative assessment of the quality of four technical models of BH saturation magnetization curve performed for four modern magnetic materials: constructional corrosion resistant steel, Mn-Zn ferrite, amorphous alloy with perpendicular anisotropy as well as Finemet-type nanocrystalline magnetic material. Presented results confirm reliability of the model as well as indicate that high-speed calculation may be done using arctangent function.

Keywords: saturation, magnetization curve, perpendicular anisotropy, Mn-Zn ferrite, Finemet

1. Introduction

Methods of modeling of the magnetic hysteresis loop are developed for over one hundred years [1]. However, process of magnetization of magnetic material is one of the most sophisticated problems connected with contemporary physics. As a result, in spite of many different approaches [2, 3, 4, 5] and the use of the most advanced numerical methods [6, 7], problem of quantitative modeling of magnetic hysteresis loop remains unsolved.

On the other hand, technical simulations oriented on simulation programs with integrated circuits emphasis (SPICE) [8], finite element method (FEM) [9] or method of the moments (MoM) [10] don't require sophisticated analyses of the shape of the hysteresis loops. To be useful for technological simulations, the model of the magnetic hysteresis loop should provide fast and reliable reproduction of the shape of B-H magnetization curve.

Such models were proposed and implemented for calculations in electrical engineering since early thirties of 20th century [10]. However, in spite of wide use for numerical simulations, quantitative analysis of quality of the most popular models seems to be still not presented from the point of view of modeling the properties of modern magnetic materials.

This paper is an approach to fill this gap. Four the most popular models of B-H saturation curve

were analyzed from the point of view of quality of the modeling of modern magnetic materials: constructional corrosion resistant steel, soft ferrite, amorphous and nanocrystalline alloy. As a result, the quality of the modeling together with its efficiency was assessed by quantitative parameters.

2. Technical B-H Saturation Magnetization Curve Models

During the investigation four of the most popular models of B-H magnetization curve were tested.

Model 1: Linear model considering the amplitude permeability μ_a and saturation flux density B_s . This model is given by the following equation:

$$B(H) = \begin{cases} B_s & \text{for } \mu_a H \geq B_s \\ \mu_a H & \text{for } -B_s < \mu_a H < B_s \\ -B_s & \text{for } \mu_a H \leq -B_s \end{cases} \quad (1)$$

Problem connected with this model is a non-linear derivative. Moreover, in the case of use of linear model in Octave/Matlab it is very important to avoid for-based loop to introduce saturation to linear model. Instead of for-based loop, the vectorisation method is recommended, as about 20 times faster solution. The example of vectorisation of equation 1 implemented in Octave is presented in the Fig. 1.

```
mi0=4.*pi.*1e-7;
Bmodel=Hmeas.*mi0.*mi;
Bmodel = max(Bmodel, (-1).*Bs);
Bmodel = min(Bmodel, Bs);
```

Fig. 1. Linear model implementation. Vectorisation of saturation up to B_s implemented in Octave

Model 2: Model given by the Langevin function describing the B-H magnetization curve in paramagnetic material [11]. This model is determined by the saturation flux density B_s and parameter a . Langevin function based model is given by the following equation:

$$B(H) = B_s \left(\coth\left(\frac{H}{a}\right) - \frac{a}{H} \right) \quad (2)$$

It should be indicated, that parameters of this model describes physical properties only for isotropic materials. However, Langevin curve can be used for

modeling of any material. In such a case parameter a doesn't describe domain wall density [12].

Model 3: Model based on the shape of arctangent function described by amplitude permeability μ_a and parameter k . Model is given by the following equation [13]:

$$B(H) = \frac{\mu_0 \mu_a}{k} \operatorname{atan}(k \cdot H) \quad (3)$$

It should be stressed that this model hasn't physical interpretation, however can quite well reproduce the shape of saturation B-H curve and has continuous derivative.

Model 4: exponential function based model [14] using saturation flux density B_s and amplitude permeability μ_a given by the following equation:

$$B(H) = B_s \left(\frac{2}{1 + e^{-\frac{2H\mu_0\mu_a}{B_s}}} - 1 \right) \quad (4)$$

Model hasn't physical interpretation, it just reproduces the shape and has continuous derivative. Moreover, typographical mistake in stating equation occurred in [14].

3. Materials for Validation of the Models

Validation of the four models was performed for the four modern magnetic materials commonly used in the industry:

Material 1: corrosion resistant martensitic steel 3H13 (X30Cr13). Such steel is used for critical components in the energetic industry.

Material 2: manganese-zinc $\text{Mn}_{0.51}\text{Zn}_{0.44}\text{Fe}_{2.05}\text{O}_4$ high permeability ferrite for power conversion applications.

Material 3: M680 type core produced by Magnetec Company, made of amorphous alloy with possibility of nanocrystallization, the NANOPERM LM ($\text{Fe}_{73.5}\text{Cu}_1\text{Nb}_3\text{Si}_{15.5}\text{B}_7$). This amorphous alloy, which exhibits strong perpendicular anisotropy is especially useful for current transformers.

Material 4: high permeability nanocrystalline $\text{Fe}_{73.5}\text{Cu}_1\text{Nb}_3\text{Si}_{13.5}\text{B}_9$ Finemet-type alloy for electronic industry

All samples were ring-shaped to avoid demagnetization.

4. Validation Procedure

Procedure of validation of the models consists of several steps, covering both experimental measurements as well as mathematical modeling:

Step 1. Experimental measurements of magnetic hysteresis loops for all four materials were carried out. For measurements the digitally controlled hysteresisgraph was used. Measurements were performed on ring-shaped samples, which were wound by magnetizing and sensing winding. Measurement uncertainty of measurements using this system was assessed as 5%.

Step 2. Parameters of the models were determined in optimization process. Target function F for optimization was determined as the sum of squares of

the differences between the results of modeling B_{model} and experimental data B_{meas} given by the following equation:

$$F = \sum_{i=1}^n (B_{meas} - B_{model})^2 \quad (5)$$

The minimization of the target function F , was carried out by the simplex search method [15].

Table 1. Results of the identification of the parameters for technical models of B-H saturation curve

Model	Material	Parameter	Value
Model 1: Linear model	Steel 3H13	B_s	1.05 T
		μ_a	464
	Mn-Zn ferrite	B_s	0.36 T
		μ_a	8737
	Amorphous alloy	B_s	1.31 T
		μ_a	4 494
	Nanocrystalline Finemet	B_s	1.15 T
		μ_a	326 743
Model 2: Langevin model	Steel 3H13	B_s	1.25 T
		a	544
	Mn-Zn ferrite	B_s	0.44 T
		a	10.0
	Amorphous alloy	B_s	1.46 T
		a	58.3
	Nanocrystalline Finemet	B_s	1.24 T
		a	0.68
Model 3: atan- function based model	Steel 3H13	k	0.0098
		μ_a	641
	Mn-Zn ferrite	k	0.053
		μ_a	12 404
	Amorphous alloy	k	0.0096
		μ_a	7223
	Nanocrystalline Finemet	k	0.83
		μ_a	527 485
Model 4: exponential -function model	Steel 3H13	B_s	1.09 T
		μ_a	564
	Mn-Zn ferrite	B_s	0.38 T
		μ_a	11 005
	Amorphous alloy	B_s	1.32 T
		μ_a	5 850
	Nanocrystalline Finemet	B_s	1.16 T
		μ_a	412 879

Table 2. Quality of the models for different soft magnetic materials

Model	Material	Parameter		
		e_{max} (%)	σ (%)	R^2
Model 1: Linear model	Steel 3H13	74	20	0.92
	Mn-Zn ferrite	27	7.8	0.98
	Amorphous alloy	7.4	1.0	0.9998
	Nanocrystalline Finemet	78	14	0.97
Model 2: Langevin model	Steel 3H13	78	21	0.92
	Mn-Zn ferrite	26	8.2	0.98
	Amorphous alloy	10	2.8	0.997
	Nanocrystalline Finemet	87	14	0.97
Model 3: atan-based model	Steel 3H13	80	21	0.92
	Mn-Zn ferrite	26	8.1	0.98
	Amorphous alloy	12	3.1	0.996
	Nanocrystalline Finemet	88	14	0.97
Model 4: exponential model	Steel 3H13	78	21	0.92
	Mn-Zn ferrite	25	8.1	0.98
	Amorphous alloy	7.3	1.8	0.9992
	Nanocrystalline Finemet	83	14	0.97

Table 3. Calculation time for B-H models (calculated for 10^6 points)

Model	Calculation time (s)
Model 1: Linear model	0.41
Model 2: Langevin model	0.59
Model 3: atan-based model	0.41
Model 4: exponential model	0.45

Step 3. Parameters determining the quality of the models were calculated for different soft magnetic materials. During the assessment following parameters were calculated:

- e_{max} (%) – maximal difference (given in percents) between the results of modeling and results of measurements

- σ (%) – mean square root of the difference (given in percents) between the results of modeling and results of measurements
- R^2 – determination coefficient.

Mathematical modeling was carried out using open-source OCTAVE 4.0.0 with *optim* toolbox 1.4.1. However, developed code is fully compatible with

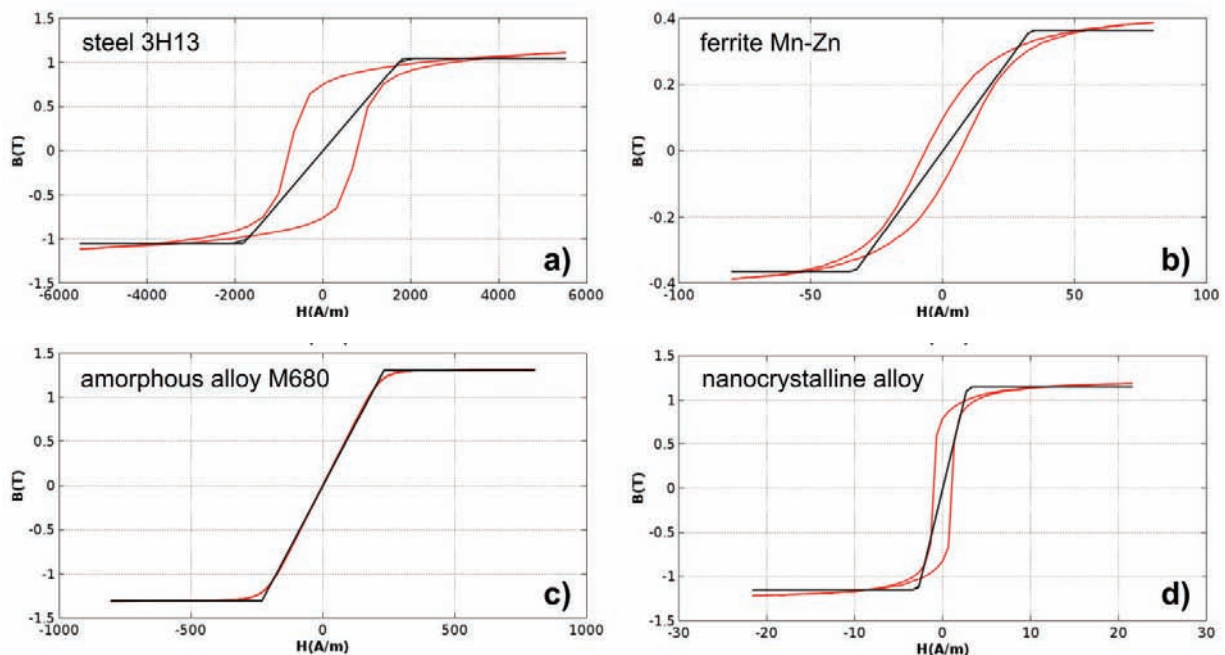


Fig. 1. Results of the fitting of linear model (model 1) for: a) steel 3H13, b) Mn-Zn ferrite, c) amorphous alloy, d) Finemet-type nanocrystalline alloy

MATLAB. To enable verification of the validation process, scripts used in presented research are available at: <http://zsisp.mchtr.pw.edu.pl/BHmodels>

5. Results

The results of the determination of model's parameters using the minimization of the target function F are presented in the Table 1. It should be indicated, that parameters, which are physically

justified (such as amplitude permeability μ_a or saturation flux density B_s) are coherent for different models. Results of the fitting of different models for tested materials may be also seen in the Figures 1–4.

Parameters determining the quality of the models for different magnetic materials are presented in the Table 2. It can be seen, that the quality of the model is mainly determined by the wideness of the hysteresis loops, whereas influence of the shape of

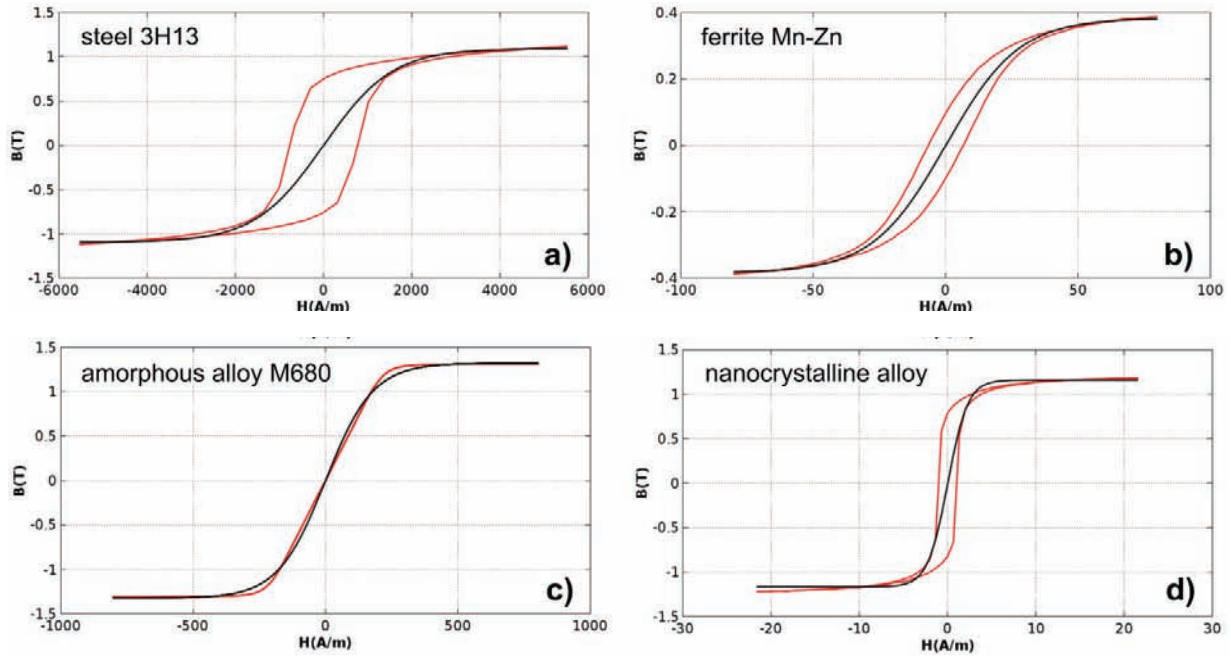


Fig. 2. Results of the fitting of Langevin function based model (model 2) for: a) steel 3H13, b) Mn-Zn ferrite, c) amorphous alloy, d) Finemet-type nanocrystalline alloy

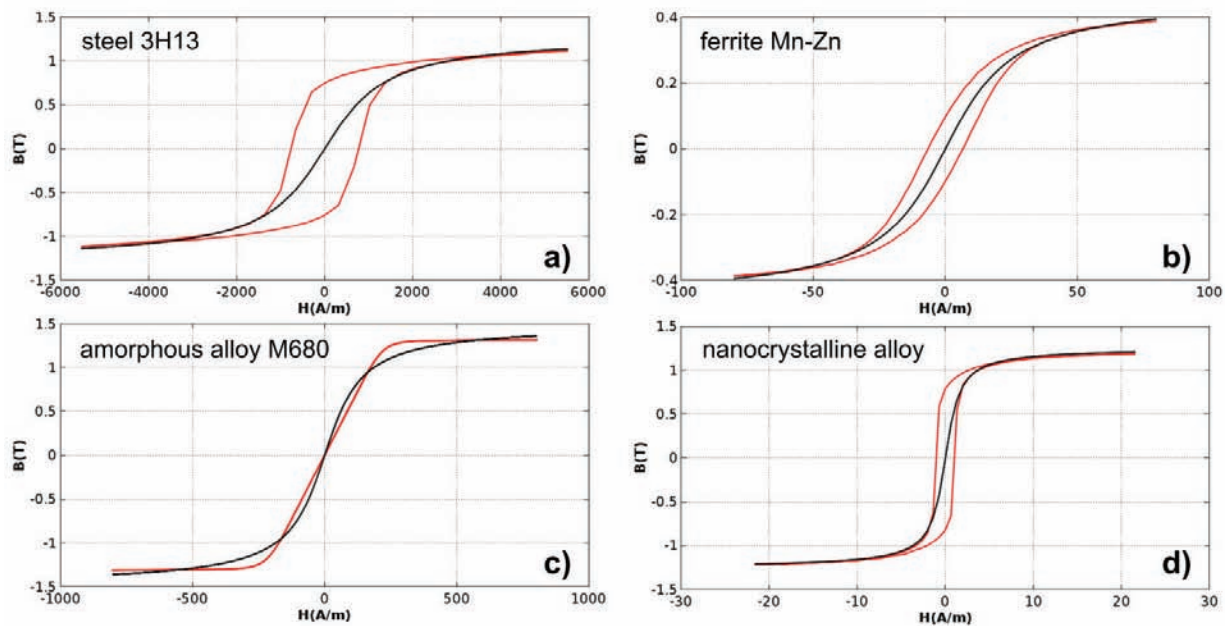


Fig. 3. Results of the fitting of arctangent function based model (model 3) for: a) steel 3H13, b) Mn-Zn ferrite, c) amorphous alloy, d) Finemet-type nanocrystalline alloy

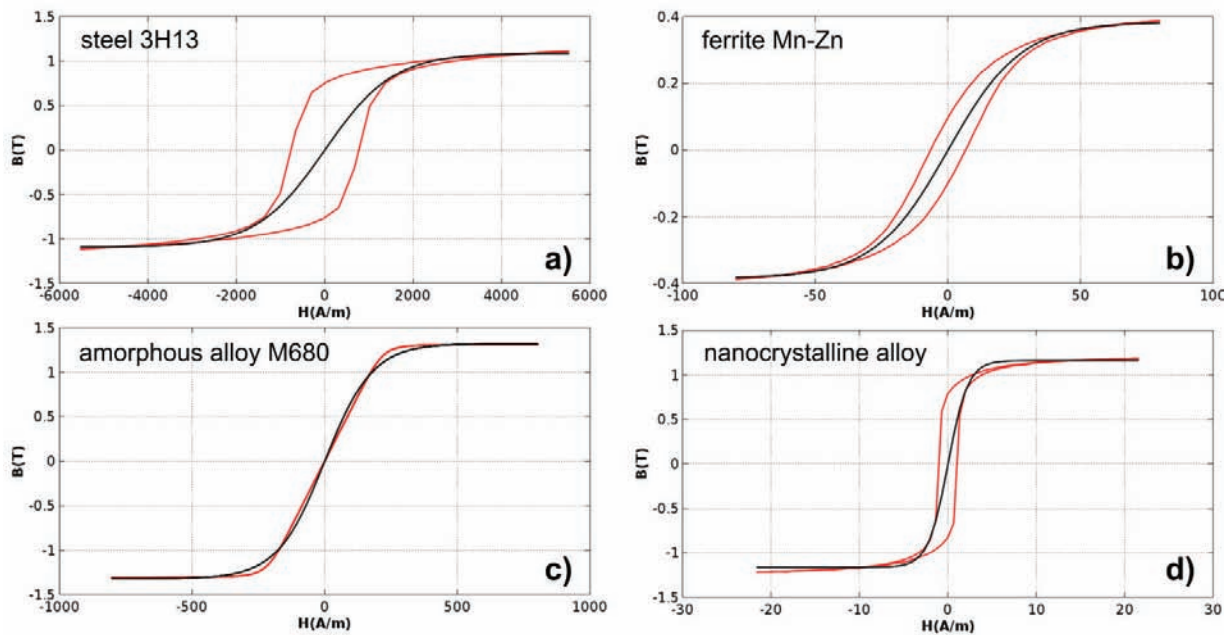


Fig. 4. Results of the fitting of exponential function based model (model 4) for: a) steel 3H13, b) Mn-Zn ferrite, c) amorphous alloy, d) Finemet-type nanocrystalline alloy

BH curve is negligible. This is especially seen in the case of amorphous alloy, where the highest values of R^2 coefficient and the best fitting was obtained.

Assessment of calculation time for different models is given in the table 3. Assessment was done for 10^6 test points and is presented in seconds. Tests were performed for Octave 4.0.0 working at MINGW32_NT-6.1 Windows 7 Service Pack 1 i686, with i5-2400 3.1GHz core.

It can be seen in Table 3, that all four models are very effective in calculation of large numbers of points of BH curve. Moreover, both linear model (model 1) and atan-based model (model 3) gives similar time for calculation.

6. Conclusions

Presented results indicate, that all four models of B-H saturation magnetization curves enables fast and reliable modeling. However, arctangent function based model (model 2) achieved similar efficiency of calculation as a linear model, which makes it especially suitable for technical simulations oriented on simulation programs with integrated circuits emphasis, finite element method or method of the moments.

Accuracy of the results of the modeling by all four models is similar and is determined mainly by the lack of the representation of magnetic hysteresis loop in B-H saturation magnetization curve. However, very good results were obtained for linear model, which makes it very useful, due to its simplicity and efficiency of calculations.

AUTHORS

Roman Szewczyk* – Industrial Research Institute for Automation and Measurements, Al. Jerozolimskie 202, 02-486 Warsaw, Poland, rszewczyk@onet.pl

*Corresponding author

REFERENCES

- [1] L. Rayleigh, "On the behaviour of iron and steel under the operation of feeble magnetic forces" *Philosophical Magazine*, vol. 23, no. 142, 1887, 225–245. DOI: 10.1080/14786448708628000.
- [2] D. C. Jiles, D. Atherton, "Theory of ferromagnetic hysteresis", *J. Magn. Magn. Mater.*, vol. 61, 1986, 48. DOI: 10.1016/0304-8853(86)90066-1.
- [3] A. Globus, „Some physical consideration about the domain wall size. Theory of magnetization mechanism”, *J. de Physique C1*, 1977, C1-1. DOI: 10.1051/jphyscol:1977101.
- [4] Vadjá F., Della Torre E., "Measurement of output dependent Preisach functions", *IEEE Trans. Magn.*, vol. 27, 1991, 4757. DOI: 10.1109/20.278938.
- [5] Augustyniak B., Degauque J., "New approach to hysteresis process investigation using mechanical and magnetic Barkhausen effects", *J. Magn. Magn. Mater.*, vol. 140–144, part 3, Feb. 1995, 187–189. DOI: 10.1016/0304-8853(94)01603-8

- [6] Kucuk I., "Prediction of hysteresis loop in magnetic cores using neural network and genetic algorithm", *J. Magn. Magn. Mater.*, vol. 305, 2006, 423. DOI: 10.1016/j.jmmm.2006.01.137.
- [7] Wilson P. R., Ross J. N., Brown A. D., "Optimizing the Jiles-Atherton model of hysteresis by a genetic algorithm", *IEEE Trans. Magn.*, vol. 37, 2001, 989. DOI:10.1109/20.917182.
- [8] A. Maxim, D. Andreu, J. Boucher, "A new analog Behavioral SPICE macromodel of magnetic components". In: *Proceedings of the IEEE International Symposium on Industrial Electronics, ISIE '97*, 1997, 183. DOI: 10.1109/ISIE.1997.648925
- [9] F. J. Perez-Cebolla, A. Martinez-Iturbe, B. Martindel-Brio, E. Laloya, S. Mendez, C. E. Montano, "3D FEM characterization of a switched reluctance motor from direct experimental determination of the material magnetization curve". In: *IEEE International Conference on Industrial Technology (ICIT)*, 2012, 19–21 March 2012, 971–976. DOI: 10.1109/ICIT.2012.6210065
- [10] Y. Takahashi, C. Matsumoto, S. Wakao, "Large-Scale and Fast Nonlinear Magnetostatic Field Analysis by the Magnetic Moment Method With the Adaptive Cross Approximation", *IEEE Transactions on Magnetics*, vol. 43, no. 4, April 2007, 1277–1280. DOI: 10.1109/TMAG.2006.890973.
- [10] J. P. Barton, "Empirical Equations for the Magnetization Curve", *Transactions of the American Institute of Electrical Engineers*, vol. 52, no. 2, June 1933, 659–664. DOI: 10.1109/T-AIEE.1933.5056367.
- [11] N.C. Pop, O.F. Caltun, "Jiles-Atherton magnetic hysteresis parameters identification", *Acta Phys. Pol. A*, 2011, 120, 491–496.
- [12] D. C. Jiles, D. L. Atherton "Ferromagnetic hysteresis", *IEEE Trans. Magn.*, vol. 19, 1983, 2183. DOI: 10.1109/TMAG.1983.1062594.
- [13] M. M. Ponjavic, M. R. Duric "Nonlinear modeling of the self-oscillating fluxgate current sensor", *IEEE Sensors Journal*, vol. 7, 2007, 1546. DOI: 10.1109/JSEN.2007.908234.
- [14] G. Mirsky, "Magnetic-Core Modeling Offers Insight into Behavior, Operating Range, Saturation", *Electronic Design*, Sep 9, 2015.
- [15] Lagarias, J.C., J. A. Reeds, M. H. Wright, P. E. Wright, "Convergence Properties of the Nelder-Mead Simplex Method in Low Dimensions", *SIAM Journal of Optimization*, vol. 9, no. 1, 112–147, 1998. DOI:10.1137/S1052623496303470.